Research Article

Based on the CT Image Rebuilding the Micromechanics Hierarchical Model of Concrete

Lei Guangyu [ID][1,2,3] **and Han Jichang**[1,2,3]

[1]*Shaanxi Land Engineering Construction Group, Xi'an 710048, China*
[2]*Institute of Land Engineering and Technology, Shaanxi Provincial Land Engineering Construction Group Co Ltd, Xi'an 710048, China*
[3]*Key Laboratory of Degraded and Unused Land Consolidation Engineering, The Ministry of Natural Resources, Xi'an 710048, China*

Correspondence should be addressed to Lei Guangyu; leiyugogo@163.com

Establishing a mesoscopic numerical model to investigate the mechanical properties of concrete has very important significance. This paper considers the random distribution of aggregate in concrete. The aggregate is assumed to be spherical, respectively, to simulate the interface layer as the entity unit or the contact elements. The random aggregate model and the interface model of random aggregate were established. Based on the CT image and the application of MATLAB and MIMICS software, the different characteristics of the concrete model for 3D reconstruction were set up. Through comparative analysis of the advantages and disadvantages of different models, considering the CT number included in the CT images, this paper establishes the reconstruction model, which includes the shape of concrete aggregates, gradation, holes, etc. The analysis results have shown that the model can infer realistic concrete behavior, providing a new approach for studying concrete properties at the mesoscale.

1. Introduction

Concrete is a composite material consisting of water, cement, and coarse aggregates. The special properties of the composite material determine its macroscopic mechanical properties [1]. The destruction process involves the interaction of various scales, from the microscopic to the macroscopic [2, 3] . Currently, the mesoscale is considered the linking bridge between the microscopic and macroscopic scales. The micromechanical numerical method, based on the finite element method, uses the concrete micromechanical model to study its failure process and obtain the intrinsic relationship between mesoscopic failure and macrodestruction, thus investigating the failure mechanism of concrete materials [4–9].

With the improvement of theoretical methods and computer hardware components, graphics processing software and meshing tools have been continuously upgraded, resulting in easier simulation of concrete mesostructures. Nowadays, using numerical methods to investigate the mechanical properties of concrete has received extensive attention from researchers. Indeed, the development of numerical models has an important influence on the simulation results. Among the most representative models in the literature are the random particle model [10], lattice model [11, 12], stochastic mechanical property model [13], and statistical damage constitutive model [14–16].

The micromechanical method is typically utilized to analyze the concrete characteristics using numerical experiments. Under the condition that the calculation model is reasonable and the material parameters of each concrete phase are sufficiently accurate, some tests can be realistically replicated to overcome the objective limitations of the test conditions and human factors [29]. This has greatly promoted the study of the mechanical properties of concrete [17]. Nevertheless, previous research has outlined some

limitations and drawbacks in the above models. At present, digital image processing technology is becoming significantly important for developing numerical models. Recently, concrete computed tomography (CT) scan image reconstruction models have become a hotspot and frontier of research on the numerical simulation of construction materials [18–21].

The real shape and location of aggregate particles in concrete were assumed in numerical analyses based on X-ray CT scans. Reference [22] found that satisfactory agreement regarding the vertical force versus crack mouth opening displacement evolution and crack geometry was achieved between analyses and laboratory tests. Two-dimensional mesoscale finite element models with realistic aggregates, cement paste, and concrete voids are developed using microscale X-ray CT images. Cohesive elements with traction-separation laws are pre-embedded within cement paste and aggregate-cement interfaces. Reference [23] simulated complex nonlinear fracture and tension tests using a large number of images. Reference [24] proposed an objective judgment criterion of unit attribute recognition based on the method of mesh mapping and established the 3D finite element model with the same aggregate proportion as the specimen in the experiment.

This study combines the literature sources' achievements over the years to develop different microscopic concrete numerical models and analyze their respective deficiencies. After that, it establishes a concrete reconstruction model based on CT images. The model considers the concrete mesostructure to simulate its behavior realistically. This study is expected to provide a reference for future investigations of the mesoconcrete's mechanical properties.

2. Mesoscopic Concrete Stochastic Model

Generally, the concrete random model is used to replicate testing samples numerically using the knowledge of the random sampling method and statistics along with the actual mixture proportions. The advantage of this approach is the ability to simulate the influence of different factors on concrete behavior. At present, the method is considered mature and independent of the data size, and its development is relatively perfect. Perform calculations on different types of specimens.

2.1. Random Aggregate Model. The random aggregate model is a three-phase heterogeneous composite consisting of aggregates, mortar, and a bond zone between the two. Previously, the Monte Carlo method was used to generate random numbers [25]. Based on the self-programmed model generation procedure, the projected grid method is used to assign the corresponding material properties according to the unit type. Due to the involvement of different material parameters in each phase, the load-deformation relationship of the concrete specimen is nonlinear. It can be used to simulate the specimen's crack propagation process and damage patterns [26].

This approach to determining the position of aggregates with different particle sizes in the sample involves calculating the number of aggregates using the actual mix ratio of concrete and assuming spherical-shaped aggregates with four variables each. The diameter of the sphere is used to distinguish the size of the aggregate, and the position of the sphere center (XYZ) is used to determine the location of the aggregate. According to the self-programming procedure, the spherical center coordinates are generated randomly using the Monte Carlo method. Generally, different spheres meet objective conditions by setting constraints and adopting a cyclical comparison method. A 3D random distribution geometric model of concrete aggregates can be obtained by compiling the generated random variables into corresponding FORTRAN programs and reading them into ANSYS in the command flow mode.

Once the concrete geometric model is generated, the aggregate, mortar, and interface are given corresponding parameters. Moreover, the material is meshed using the finite element method to obtain a 3D random distribution model of concrete aggregates. The overall model diagram is shown in Figure 1, and the section diagram is shown in Figure 2.

2.2. Random Aggregate Contact Surface Model. The concrete's random aggregate contact surface model is a two-phase material that consists of mortar and aggregate and uses an ANSYS contact surface unit to simulate their interface joint. This method starts by establishing a concrete cylinder body in ANSYS, then randomly generating aggregate spheres in the entity using the self-programming procedure to separate the cylinder and aggregate spheres for the BOOLEANS calculations. The position of the aggregate formed at this time is a hollow concrete specimen. Use the program again to read the position coordinates of the aggregate and generate its entity. The overall mesh is typically selected using the SOLID45 element. Besides, the aggregate projection grid method is used to distinguish the fundamental material properties. Moreover, the contact elements between the aggregate and the mortar are defined using the TARGE170 and CONTA174 unit types [27]. The model contact element is shown in Figure 3, and the cross-section of the random aggregate contact surface model is shown in Figure 4.

Compared with the random aggregate model, this technique uses a contact element instead of an interface element, resulting in considerably lower computational time and cost. The results of the two calculations are shown in Figure 5. It can be seen that their destruction rules are the same, indicating that the random aggregate contact surface model can be a good substitute for the random aggregate model.

3. Mechanical Model Based on Three-Dimensional Reconstruction of Concrete Images

Due to the difference between the random model and the actual concrete internal structure, the research and analysis cannot lead to a complete correspondence with the test. Therefore, studying the mechanical model based on concrete
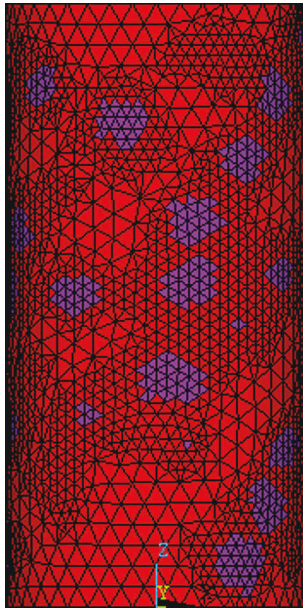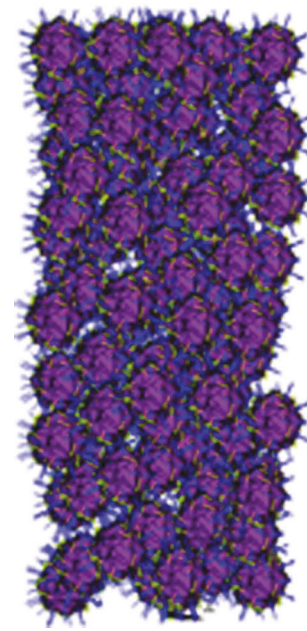
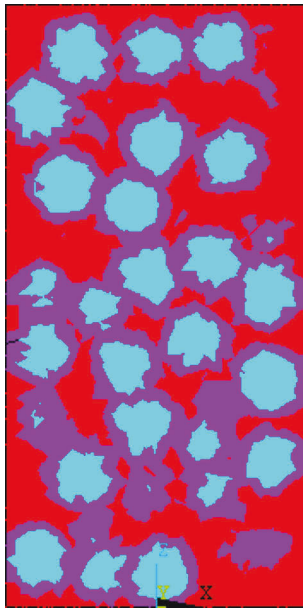FIGURE 1: Model of random aggregate.

FIGURE 2: Section of random aggregate.
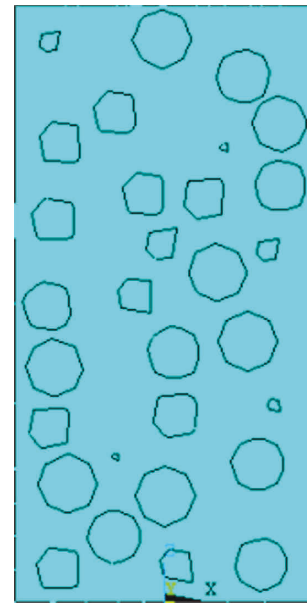

FIGURE 3: Contact element of model.

FIGURE 4: Section of the contact element.

images for 3D reconstruction has gradually gained attention and progress. The 3D reconstruction model is a model that is closer to the mesostructure of the actual concrete and is an important foundation for future research on the mechanical properties of mesoconcrete.

3.1. Three-Dimensional Reconstruction Model of Concrete Based on the Joint Unit Method. Unlike previously explained techniques, the three-dimensional reconstruction model is closer to the real mesostructure of concrete and can be compared with the physical experiment. The 3D finite element model of concrete based on the joint-element method abandons the modeling order of points, lines, surfaces, and bodies by discretely separating the concrete into many nodes in the space, which are then connected to generate the unit. Then the material properties of the specimen are determined from the elements containing the node attributes, thereby establishing a 3D finite element model of the concrete mesostructure. The modeling procedure in this method is described as follows:

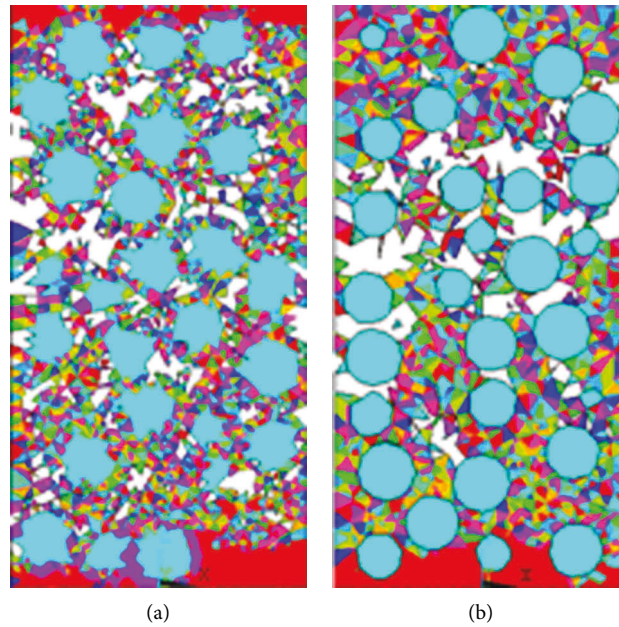(1) Each CT image is processed to save its CT number and spatial position as a cross-section file.

(a)   (b)

FIGURE 5: Different damaged sections of the model. (a) Model of random aggregate. (b) Interface model of random aggregate.

(2) The image quality is enhanced using the threshold segmentation method to distinguish the aggregate from the mortar.

(3) The image information is saved as a two-dimensional matrix using MATLAB.

(4) The pixel attribute value matrix in MATLAB is read into the ANSYS array using a self-programming code to generate a model.

The model is shown in Figure 6.

On the other hand, this method cannot yet rebuild a complete concrete test piece due to using many elements. In order to reduce the amount of data, the influence of holes, small aggregate particles, etc., is not taken into account in the reconstruction process, resulting in relatively low simulation accuracy.

3.2. Three-Dimensional Reconstruction Model of CT Images Based on MIMICS Software. Some large-scale image creation and editing software, such as MIMICS, has a 3D entity reconstruction function. MIMICS software can directly read Dicom format CT scan images through the following procedure:

(1) Interpolate the picture using image positioning.

(2) set different thresholds for different materials.

(3) modify the pixels of the image by different pixel modification methods.

(4) once each layer of the image is processed to remove redundant data, a 3D geometric concrete model can be established based on the calculation.

(5) use ANSYS software to read the list file of the 3D concrete built in the MIMICS software and generate the finite element model directly.

The overall model is shown in Figure 7,

Based on the concrete reconstruction model obtained from the above CT images, a complete calculation cannot be performed at present due to the model's large number of elements and relatively low accuracy.

4. Key Issues and Technical Approaches to Concrete Micromechanical Models

The numerical model of mesoconcrete is the basis for studying the material's mechanical properties. The diversity in the concrete's constituent materials and the randomness in the preparation process increase the complexity and nonuniformity of the model compared to other materials. Therefore, there are many key problems in the numerical model of the mesoconcrete. At present, this method cannot perform one-to-one comparative analysis with physical tests because the simulated aggregate shape and position are different from those of real concrete specimens, and the model rarely considers the influence of holes in the specimen. The 3D reconstruction model of concrete relies on CT images. Based on the digital image processing method and large-scale image processing software for finite element modeling, the mesostructure of the real specimen is well simulated. The advantage of this method is that, according to the actual concrete shape, a consistent finite element model can be generated to perform concrete mechanical tests better. Accordingly, the development of concrete reconstruction models is the direction of future concrete property investigations. This research topic is still facing some deficiencies. For instance, image information data compression results in large amounts of data that cause the completeness of a full model computation to be prevented. Moreover, the model's accuracy is low due to the unit selection of feature points. Besides, the model cannot
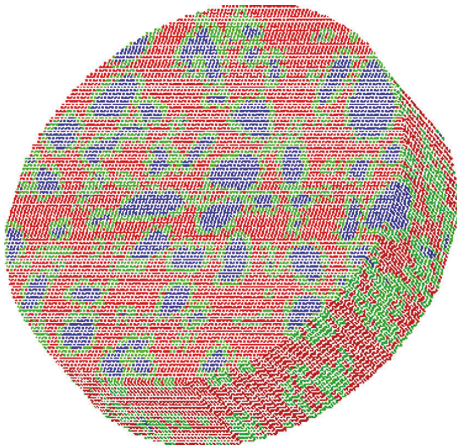
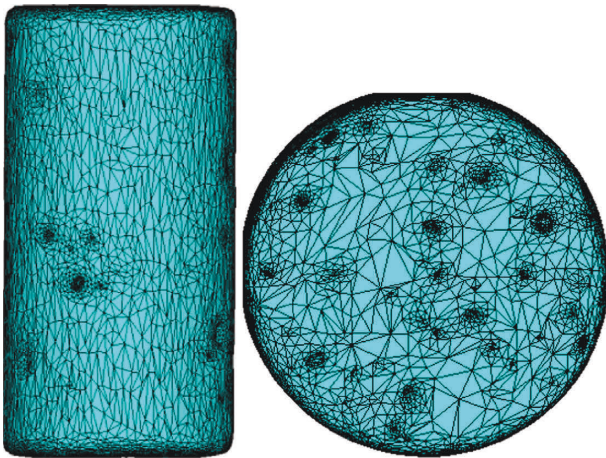FIGURE 6: The specimen FEM elements.

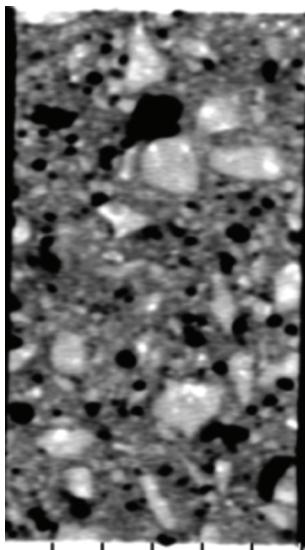FIGURE 7: 3D FEM elements of concrete.

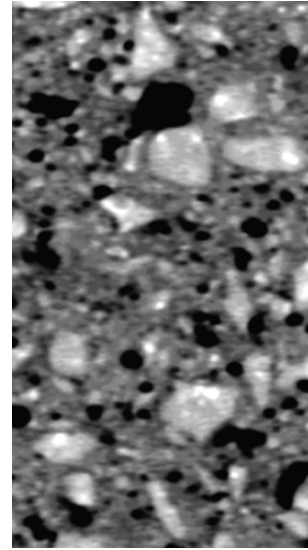
FIGURE 8: Initial graph of the CT section.

FIGURE 9: After extraction of the CT section.

consider the impact of small aggregates, holes, and other factors during the reconstruction process. These factors have an important influence on the mechanical properties of concrete. Combining the above problems with the concrete random model and the concrete reconstruction model, the common limitation of the two is that the influence of small volume components such as holes and fine aggregates has not been taken into account, along with the influence of different aggregate parameters. These are problems that cannot be ignored in the study of concrete mechanics. Accordingly, a concrete mesoscopic model that reflects actual conditions is the basis for investigating concrete mechanical properties and obtaining reasonable and correct results. Therefore, based on the problems existing in the above models, starting from concrete CT images, reconstructing the concrete mechanical model, taking into account the influence of different aggregate parameters and concrete holes, reflecting these characteristics in the reconstruction model is the trend to study the numerical calculation model of the microscopic concrete.

5. Microscopic Concrete Reconstruction Model Based on CT Number

The CT machine scans the concrete sample layer by layer to obtain CT slices of any scanned surface inside the concrete. Each slice contains the material information and density of the layer. Finally, the material properties can be represented by the CT values of each pixel [28].

5.1. Image Processing. In a single test specimen, the number of CT digital regions and the number of scanned CT slices vary due to the difference in the resolution of the CT machine and the scanning thickness. Before processing an image, it is first necessary to determine the resolution of the image and the geometric location of the CT slice in the
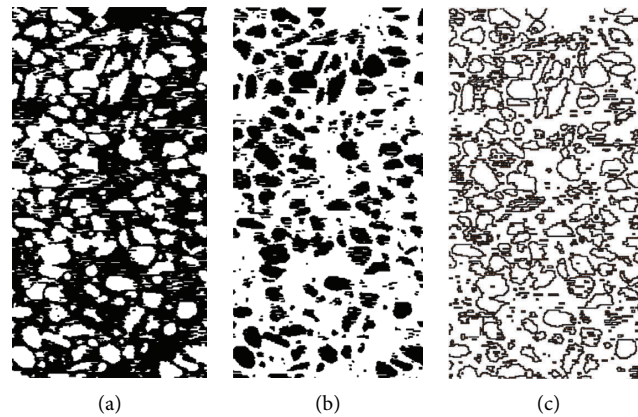
FIGURE 10: Profile of every material in the CT section after reconstruction. (a) Mortar. (b) Aggregate. (c) Interface.

concrete specimen, and then select the CT slice that needs to be reconstructed. At the same time, since the CT machine scans the concrete specimens and the parts around the specimens, CT slice images also contain this information. The image is first divided into study areas, and the areas that need to be investigated for reconstruction are selected. A raw CT slice map is shown in Figure 8. The figure contains the scanned parts of the test specimen and the information on the surrounding blank parts. In the analysis, if the CT image is not processed, it will cause errors when analyzing the image data. Therefore, the image study area is extracted, as shown in Figure 9.

Once the extraction of the CT slice image is completed, the size of the image should be determined to obtain the pixel matrix of the image. Then use the ENVI software to extract the CT value at each pixel. At this point, the coordinate value at the pixel point and the CT value are in a one-to-one correspondence and represent the material information at this position. For the convenience of calculation and statistics, CT values are normalized. Thereafter, the position information and material quantity are determined. Finally, the data, including the position coordinates of the aggregate, mortar, and holes and the size of the CT value, is saved.

5.2. Model Reconstruction. The ABAQUS software generated a two-dimensional geometric model with the same dimensions as the CT slices. The two-dimensional plane geometry model was meshed. Each unit represented a pixel, and the ".inp" file was proposed once the partition was completed. According to the Fortran language, the corresponding program is compiled, and the node information in the ".inp" file is replaced with the information of the node coordinates of the aggregate, mortar, and hole in the CT slice, and the file is saved and read again. At this point, the information contained in the model's elements and nodes are the aggregates, mortar, and hole information. In this study, a new unit was added between the aggregate and the mortar, considered a transitional layer, giving it corresponding material properties. The reconstruction of the
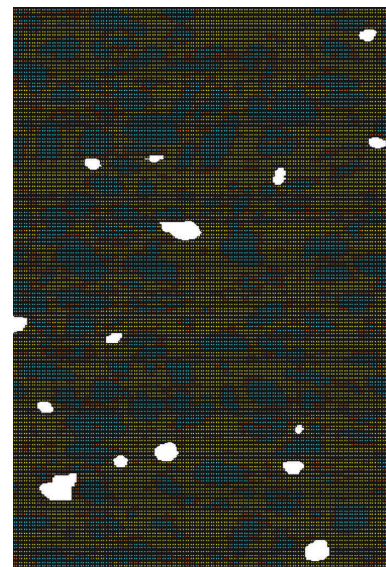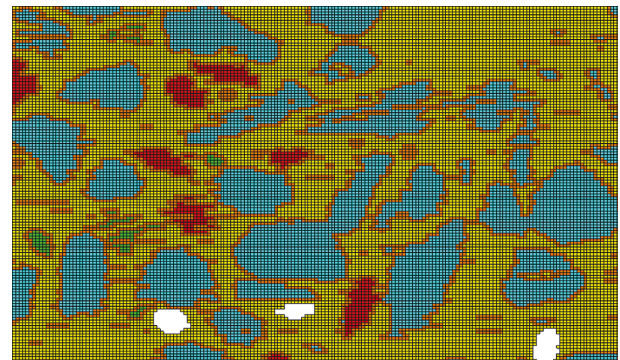

FIGURE 11: Whole reconstruction model.

FIGURE 12: Reconstruction partial enlarged.

model is complete. Each material section is shown in Figure 10, and the whole is shown in Figure 11.

After selecting the image and processing the data, the CT image is finally converted into a numerical model. It can be seen from the partial enlargement of Figure 12 that the

reconstructed model contains aggregates, interfaces, mortar, and holes at all levels.

This model integrates the characteristics of the random models and CT reconstruction techniques. The interface influence in the random model and the aggregate shape and gradation effects in the CT reconstruction model were taken into account, and the influence of holes that both models did not consider was increased.

In order to verify the rationality of the model, a mechanical analysis was performed under pressure and tensile loads. This paper used the plastic damage model of concrete. The damage factor D is calculated separately according to the compression and tension conditions. The mechanical parameters of each material are shown in Table 1. This paper applied dynamic compression and tension forces using a displacement-controlled protocol. The loading curve is shown in Figures 13 and 14. The dynamic compression loading time was 0.1 s, and the loading displacement was 1 mm. Besides, the loading time for the dynamic tensile case was 0.05 s, and the loading displacement was 0.12 mm.

5.3. Pressure Load. The dynamic pressure load is applied to the model top, and the bottom surface of the model is restrained. The computation results are shown in Figures 15 and 16. In the initial loading stage, when the specimen is not damaged, the displacement of the material changes regularly, where the top displacement is the largest, the bottom is the smallest, and the layering changes sequentially. When the specimen is destroyed, the displacement varies locally. Under the dynamic pressure load, the damage starts at the top ends of the specimen. As the load increases, the damage range gradually expands over the whole section. When the stress reaches a certain value, damage in some areas begins to increase and gradually penetrate, and finally, several macroscopic cracks penetrating the entire specimen are formed. It can be seen from the figure that the hole has a certain impact on the concrete damage where the stress concentration is easy to occur first around the hole, causing the damage to initiate. Moreover, the hole influences the development of the damage path and affects the final failure surface.

Figure 17 shows the analysis of different materials' damage. It can be seen that the crack is mainly developed along the intersection of the mortar and the aggregate. Two major failure cracks can be observed in the mortar, indicating that the crack mainly occurs. The damage diagram of the interface is slightly amplified in Figure 18, where it suffered damage, and some interfaces collapsed. However, because the interface is relatively small, thin, and isolated, it cannot form a unified damage surface. Therefore, from an overall point of view, the damage mainly occurs in the mortar. However, in the initial damage stage, crack initiation starts at the interface, and when the damage accumulates to a certain extent, due to the interaction of stress between the interface, aggregate, mortar, and holes, the cracks begin to develop and penetrate. In addition to the mortar, some aggregates have experienced damage. The partial damage enlargement shows that most cracks propagate around the

TABLE 1: Material parameters.

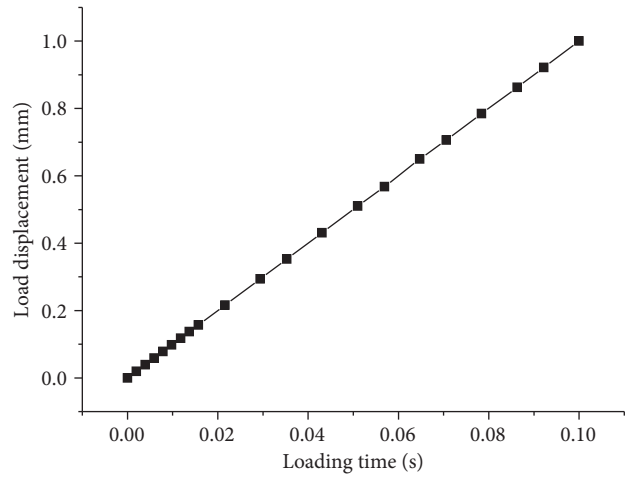| Material	Elastic modulus/ Pa	Poisson's ratio	Tensile strength/ Pa
Aggregate	5.8731×10^{10}	0.2407	$9.25e6$
Mortar	1.7458×10^{10}	0.1960	$2.78e6$
Interface	1.3967×10^{10}	0.2000	$1.56e6$

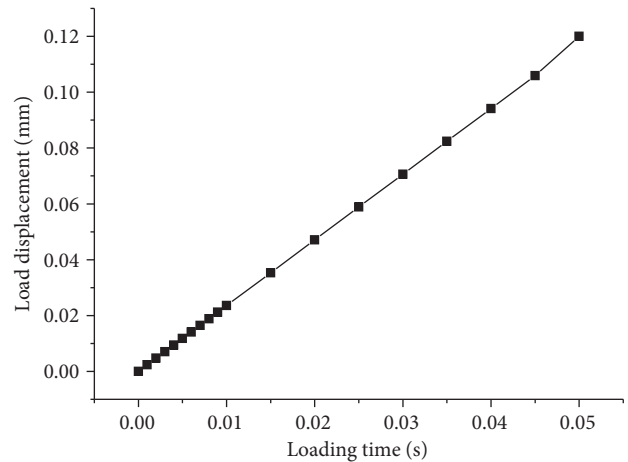FIGURE 13: The load curve of dynamic pressure load.

FIGURE 14: The load curve of dynamic tensile load.

aggregate, but some of them pass through the aggregate particles. Therefore, under the dynamic pressure load, the concrete as a composite material has a complicated failure process, and each material's stress interaction determines the cracks' development.

5.4. Tensile Load. This study applies the dynamic tensile load to the model top while its bottom surface is restrained. The analysis results are shown in Figures 19 and 20. It can be seen that when a concrete specimen is subjected to a dynamic tensile load, its failure mode is completely different from that of a dynamic compression load. For instance, it can be observed that at the beginning of the loading, the specimen's
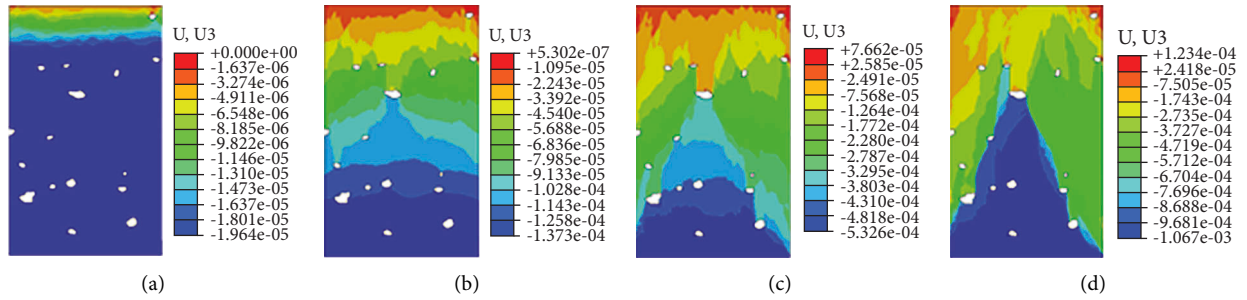
FIGURE 15: Vertical displacement graphs under different loading displacement. (a) $s = 0.02$ mm. (b) $s = 0.137$ mm. (c) $s = 0.533$ mm. (d) $s = 1$ mm.
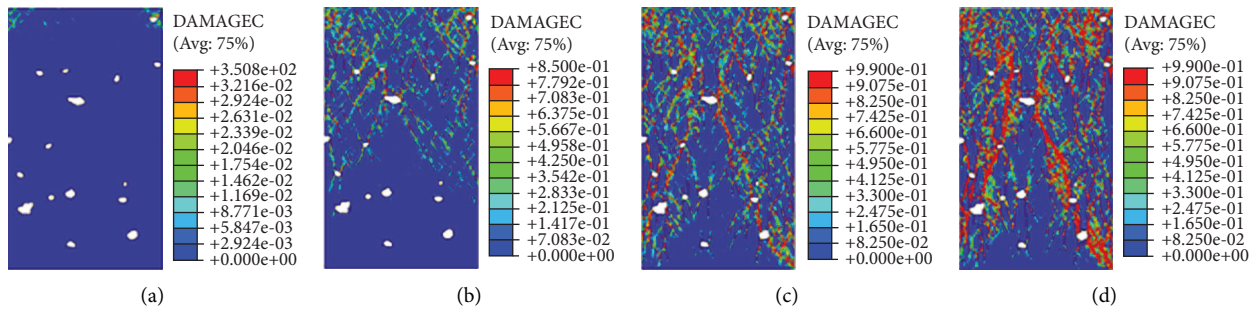

FIGURE 16: Damage failure graphs under different loading displacement. (a) $s = 0.02$ mm. (b) $s = 0.137$ mm. (c) $s = 0.533$ mm. (d) $s = 1$ mm.
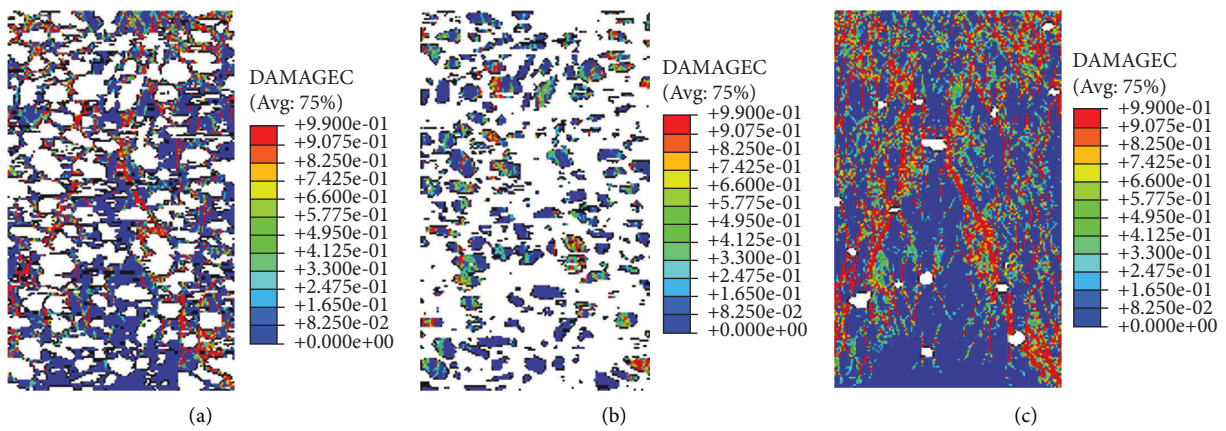

FIGURE 17: Damage graphs of different materials when the loading displacement is 1 mm. (a) Mortar. (b) Aggregate. (c) Concrete.
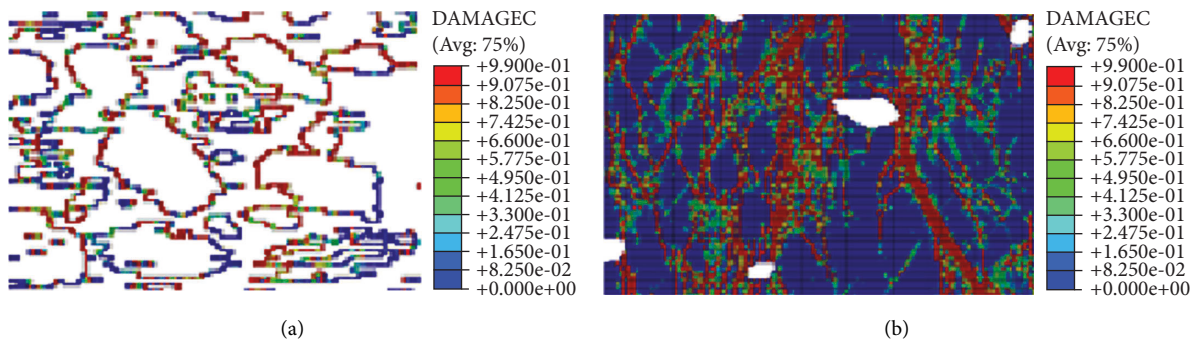

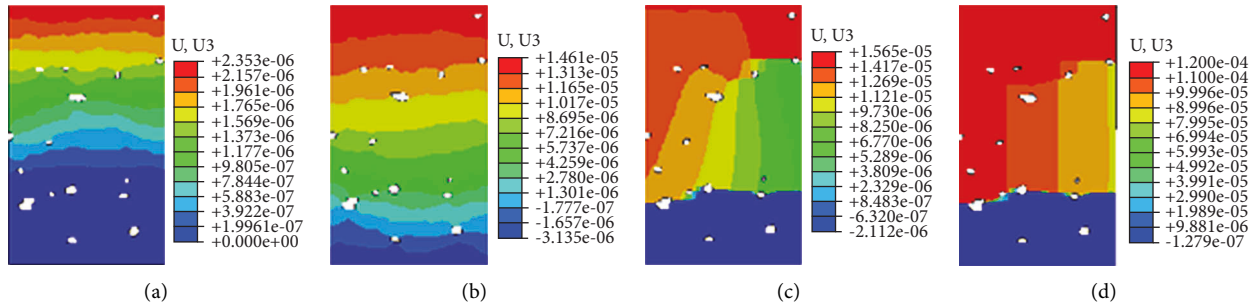FIGURE 18: Local failure graph of material. (a) Interface. (b) Concrete.

FIGURE 19: Vertical displacement graphs under different loading displacement. (a) s = 0.002 mm. (b) s = 0.015 mm. (c) s = 0.016 mm. (d) s = 0.12 mm.
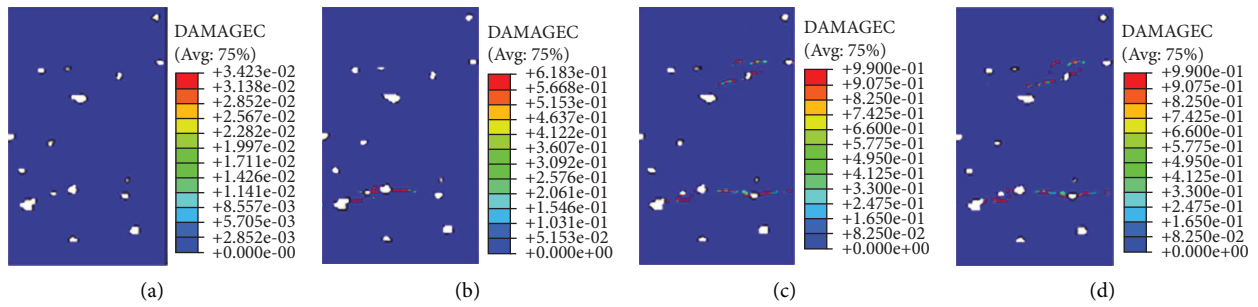

FIGURE 20: Damage failure graphs under different loading displacement. (a) s = 0.002 mm. (b) s = 0.015 mm. (c) s = 0.016 mm. (d) s = 0.12 mm.
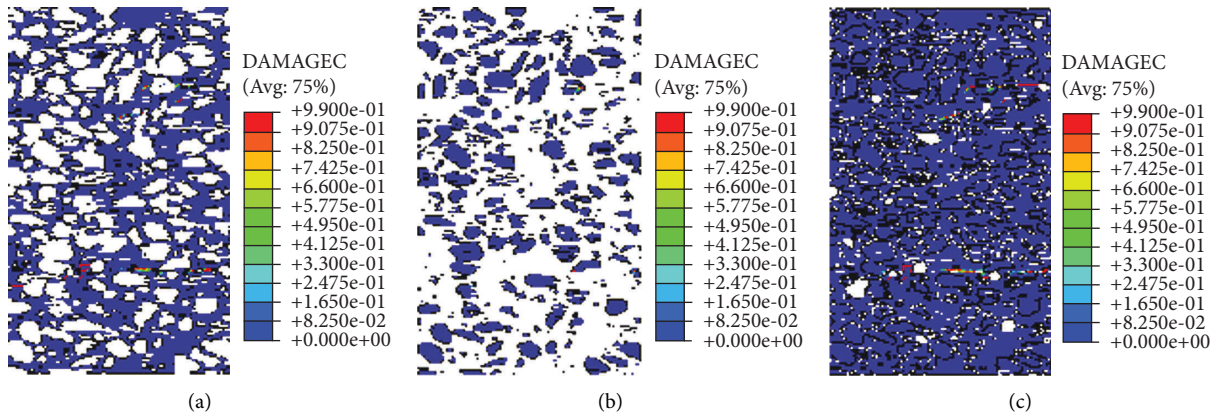

FIGURE 21: Damage graphs of different materials when the loading displacement is 0.12 mm. (a) Mortar. (b) Aggregate. (c) Concrete.

top displacement changed the most, and the damage did not occur. As the load increases, the change in displacement fluctuates, and the damage slowly develops. The vertical displacement begins to change unevenly, and the damage begins to occur slowly. Initially appearing around the hole, continuing to load, the damage begins to develop and gradually forms a damaged area throughout the specimen and perpendicular to the direction of loading. At the same time, there is intermittent damage in other parts of the test piece. When the loading reaches a certain value, the displacement has a significant mutation, indicating the occurrence of a complete collapse. From Figure 20, the degree of the damaged area throughout the specimen is more serious, and the damage accumulation eventually leads to the

destruction of the specimen, while one fracture surface runs through the specimen.

Further analysis of the mechanical changes of various materials during the stress process. As shown in Figure 21, the damage mainly occurs in the mortar, and there are many cracks under the dynamic pressure load, but there is only one main crack under the dynamic tensile load where the aggregate has slight damage. The failure surface from the overall damage figure is relatively straight and passes through part of the aggregate and most of the mortar. The interface has also suffered damage, mainly concentrated at the location of the failure surface, as shown in Figure 22. In the partially enlarged view of the overall damage, it can be clearly seen that the crack passes through small aggregate,

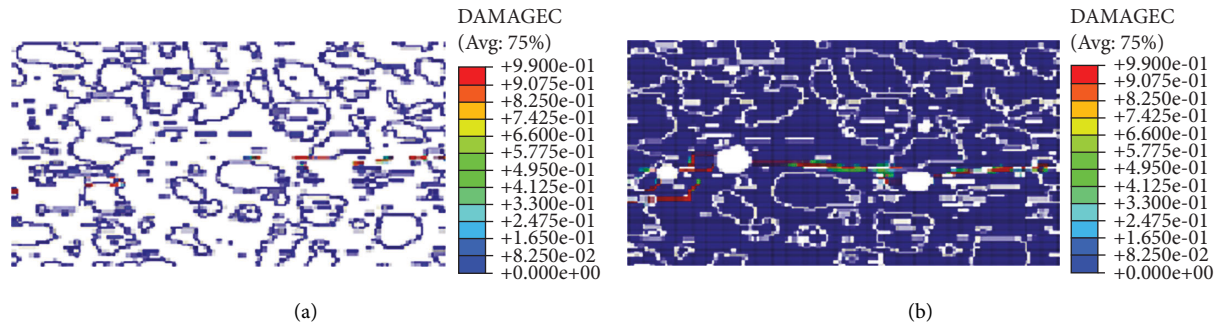(a)   (b)

FIGURE 22: Local failure enlarged graph of material. (a) Interface. (b) Concrete.

mortar, and their interface, stops at the hole, and forms on its other side.

6. Model Verification

6.1. Dynamic Pressure Test Results. The CT scanned sections under dynamic compressive load show that the concrete specimens' damage occurs abruptly. As a result, unlike damage characteristics under static pressure, it is difficult to capture the microcrack initiation process, propagation, and final development using CT. Figure 23 and 24 show the final failure modes. It can be seen that under dynamic pressure, the damaged area is large, the damage is relatively complete, the aggregate is destroyed, and the damage is "double cone" extrusion damage.
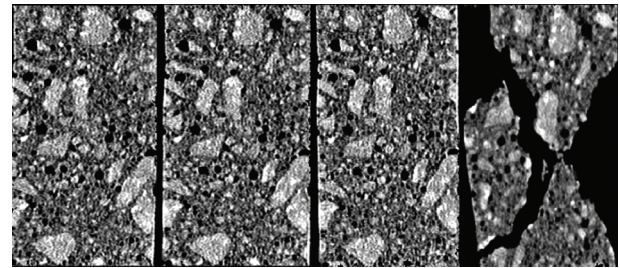
6.2. Dynamic Tensile Test Results. The CT scanning section of the concrete specimen (Figure 25) shows that the concrete specimen's damage specimen occurs suddenly under dynamic tensile load. Before the damage, each loading stage's CT image remained unchanged. After the damage, a horizontal main crack was formed in the weakest section of the whole specimen, and the crack passed through part of the aggregate. As shown in Figure 26, the fracture surface is relatively flat, the aggregate is divided into two parts, the two specimens after the failure are completed, and the concrete surface is intact.

The numerical calculation of the CT reconstruction model shows that under the dynamic load, the model's simulation results and the experimental ones from the CT test have a high similarity. The crack is mainly developed along the intersection of the mortar with the aggregate. Additionally, some aggregates are damaged, and the hole has a certain influence on the development path of the crack. There are many cracks under dynamic pressure load with a high failure degree, a large failure area, and a double cone failure. On the other hand, there is one crack only under the dynamic tensile load, the fracture surface is relatively flat, and the failure mode is the fracture surface perpendicular to the loading direction. Compared with the CT test, in which the development of cracks before failure cannot be observed due to the limitations of test conditions, the numerical tests can solve this problem by their calculation characteristics. It can be observed that the initiation and development path of

FIGURE 23: CT scan sectional drawings.

FIGURE 24: The failure of specimens under dynamic pressure.
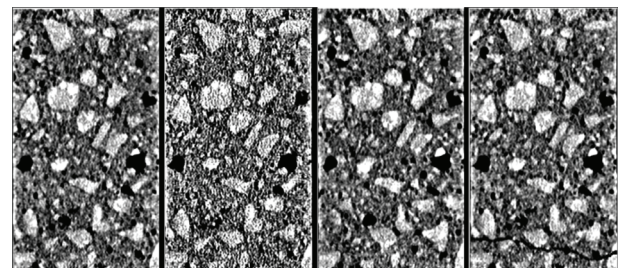

FIGURE 25: CT scan sectional drawings.

internal cracks in the concrete specimens occurs under the action of force in real-time.

Numerical experiments and CT physics tests are complementary. By establishing a numerical reconstruction model of mesoconcrete based on CT images, the two are well combined to provide effective help for further study of the mesomechanical mechanism of concrete.

FIGURE 26: The failure of specimens under dynamic tensile.

7. Conclusion

As the basis of numerical experiments, numerical models have a crucial influence on the simulation test results. Therefore, choosing a suitable numerical model is critical for obtaining accurate results.

This paper develops a reconstruction model based on CT images to perform the mechanical analysis. The results of CT experiments are compared and verified, and the main conclusions are as follows:

(1) Both the random aggregate model and the random aggregate interface model can simulate the force characteristics of the mesoconcrete. When simulating the bond between the aggregate and the mortar in the concrete, the interface elements in the random aggregate model are relatively thick, and the contact parameters in the random aggregate contact surface model are not easily determined. Besides, both models do not consider aggregate shape and hole influence.

(2) The 3D reconstruction models based on the joint-element method and the MIMICS CT image are closer to the actual concrete behavior than the random aggregate model. This observation is mainly attributed to the low precision and the lack of consideration of the unit compression. As a result, a complete primary mechanical analysis cannot be performed at present.

(3) The CT image reconstruction model based on CT number considers the aggregate gradation influence, including the shape and hole, to provide the advantages of the random aggregate model, thus achieving realistic concrete behavior compared to other models.

(4) The damage to concrete is affected by the hole, and the location of the hole is prone to cracking. Moreover, the initiation of cracks often occurs at the interface and eventually extends through the mortar. The strength of its weak specimen parts mainly determines the strength of concrete [29].

Data Availability

All data, models, and code generated or used during the study are included in the article.

Conflicts of Interest

The authors declare that they have no conflicts of interest.

Acknowledgments

References

[1] Z. W. Qu, Z. H. Liu, R. Z. Si, and Y. Zhang, "Effect of various fly ash and ground granulated blast furnace slag content on concrete properties: experiments and modelling," *Materials*, vol. 15, no. 9, p. 3016, 2022.

[2] S. Afroz, Y. D. Zhang, Q. D. Nguyen, T. Kim, and A. Castel, "Effect of limestone in General Purpose cement on autogenous shrinkage of high strength GGBFS concrete and pastes," *Construction and Building Materials*, vol. 327, Article ID 126949, 2022.

[3] Q. D. Nguyen, S. Afroz, Y. D. Zhang, T. Kim, W. Li, and A Castel, "Autogenous and total shrinkage of limestone calcined clay cement (LC3) concretes," *Construction and Building Materials*, vol. 314, no. 12, Article ID 125720, 2022.

[4] I. Carol, C. M. López, and O. Roa, "Micromechanical analysis of quasi-brittle materials using fracture-based interface elements," *International Journal for Numerical Methods in Engineering*, vol. 52, no. 12, pp. 193–215, 2001.

[5] F. Dupray, Y. Malecot, L. Daudeville, and E. Buzaud, "A mesoscopic model for the behaviour of concrete under high confinement," *International Journal for Numerical and Analytical Methods in Geomechanics*, vol. 33, no. 11, pp. 1407–1423, 2009.

[6] S. M. Kim and R. K. A. Alrub, "Meso-scale computational modeling of the plastic-damage response of cementitious composites," *Cement and Concrete Research*, vol. 41, no. 3, pp. 339–358, 2011.

[7] S. Shahbeyk, M. Hosseini, and M. Yaghoobi, "Mesoscale finite element prediction of concrete failure," *Computational Materials Science*, vol. 50, no. 7, pp. 1973–1990, 2011.

[8] M. Du, L. Jin, and D. Li, "Mesoscopic simulation study of the influence of aggregate size on mechanical properties and specimen size effect of concrete subjected to splitting tensile loading," *Engineering Mechanics*, vol. 34, no. 9, pp. 54–62, 2017.

[9] W. Wang, Z. Yi, B. Tian, Y. Zhang, and S. Lu, "Nonlinear finite element analysis of PBL shear connectors in hybrid structures," *Structures*, vol. 33, no. 10, pp. 4642–4654, 2021.

[10] G. D. Schutter and L. Taerwe, "Random particle model for concrete based on delaunay triangulation," *Materials and Structures*, vol. 26, no. 2, pp. 67–73, 1993.

[11] E. Schlangen and E. J. Garboczi, "Fracture simulations of concrete using lattice models: computational aspects," *Engineering Fracture Mechanics*, vol. 57, no. 2–3, pp. 319–332, 1997.

[12] J. P. B. Leite, V. Slowik, and H. Mihashi, "Computer simulation of fracture processes of concrete using mesolevel models of lattice structures," *Cement and Concrete Research*, vol. 34, no. 6, pp. 1025–1033, 2004.

[13] C. A. Tang and W. C. Zhu, *Numerical Simulation Tests of Concrete Damnification and Fracture*, Science Press, Beijing, China, 2003.

[14] A. R. Mohamed and W. Hansen, "Micormechanical modeling of crack-aggregate interaction in concrete materials," *Cement and Concrete Composites*, vol. 21, no. 5/6, pp. 349–359, 1999.

[15] W. F. Bai, J. Y. Chen, and S. L. Fan, "Statistical damage constitutive model for concrete material under uniaxial compression," *Journal of Harbin Institute of Technology*, vol. 17, no. 3, pp. 338–344, 2010.

[16] H. F. Ma, H. Q. Chen, and C. L Yang, "Numerical tests of meso-scale damage mechanism for full graded concrete under complicated dynamic loads," *China Civil Engineering Journal*, vol. 45, no. 7, pp. 175–182, 2012.

[17] X. L. Du and L. Jin, "Meso-element equivalent model for macro-scopic mechanical properties analysis of concrete materials," *Chinese Journal of Computational Mechanics*, vol. 29, no. 5, pp. 654–661, 2012.

[18] K. Gopalakrishnan, H. Ceylan, F. Inanc, and M. Heitzman, "Characterization of asphalt materials using X-ray high-resolution computed tomography imaging techniques," in *Proceedings of the 2006 T&DI Airfield and Highway Pavement Specialty Conference*, pp. 437–454, Atlanta, Georgia, May 2006.

[19] Q. Dai, "Two- and three-dimensional micromechanical viscoelastic finite element modeling of stone-based materials with X-ray computed tomography images," *Construction and Building Materials*, vol. 25, no. 2, pp. 1102–1114, 2011.

[20] I. Onifade, D. Jelagin, A. Guarin, B. Birgisson, and N. Kringos, *Asphalt Internal Structure Characterization with X-Ray Computed Tomography and Digital Image Processing*, pp. 139–158, Springer, Netherlands, 2013.

[21] Ł. Skarżyński, M. Nitka, and J. Tejchman, "Modelling of concrete fracture at aggregate level using FEM and DEM based on X-ray μCT images of internal structure," *Engineering Fracture Mechanics*, vol. 147, pp. 13–35, 2015.

[22] W. Trawiński, J. Tejchman, and J. Bobiński, "A three-dimensional meso-scale modelling of concrete fracture, based on cohesive elements and X-ray μCT images," *Engineering Fracture Mechanics*, vol. 189, 2018.

[23] W. Y. Ren, Z. Yang, R. Sharma, C. Zhang, and P. J. Withers, "Two-dimensional X-ray CT image based meso-scale fracture modelling of concrete," *Engineering Fracture Mechanics*, vol. 133, pp. 24–39, 2015.

[24] W. Qin and C. B. Du, "Meso-level model of three-dimensional concrete based on the CT slices," *Engineering Mechanics*, vol. 29, no. 7, pp. 186–193, 2012.

[25] N. Metroplis and S. U. Lam, "Monte Carlo method," *Ameriean: J. Amer.states*, vol. 44, no. 247, pp. 335–341, 1949.

[26] Y. N. Zheng, *Three-Dimensional Numerical Simulation on Mesolevel and CT Experiment Verification of Failure Process in Concrete*, Xi'an University of Technology, Xi'an, China, 2005.

[27] X. Y. Liang, F. N. Dang, and W. Tian, "Study on numerical model of concrete based on 3D meso-mechanics," *Chinese Journal of Applied Mechanics*, vol. 28, no. 2, pp. 129–134, 2011.

[28] G. Y. Lei, J. C. Han, and Y. Zhang, "Based on the CT image rebuilding the micromechanics hierarchical model of concrete," *Journal of Hydroelectric Engineering*, vol. 35, no. 3, pp. 105–112, 2016.

[29] Y. D. Zhang, S. Afroz, Q. D. Nguyen et al., "Analytical model predicting the concrete tensile stress development in the restrained shrinkage ring test," *Construction and Building Materials*, vol. 307, Article ID 124930, 2021.